

Vinyl C–F Cleavage by Os(H)₃Cl(PⁱPr₃)₂

German Ferrando-Miguel, Hélène Gérard, Odile Eisenstein,* and Kenneth G. Caulton*

Department of Chemistry, Indiana University, Bloomington, Indiana 47405-7102, and LSDSMS, UMR 5636, Université Montpellier 2, 34095 Montpellier, France

Received May 24, 2002

Os(H)₃ClL₂ (L = PⁱPr₃) reacts at 20 °C with vinyl fluoride in the time of mixing to produce OsHFCl(≡CCH₃)L₂ and H₂. In a competitive reaction, the liberated H₂ converts vinyl fluoride to C₂H₄ and HF in a reaction catalyzed by Os(H)₃ClL₂. A variable-temperature NMR study reveals these reactions proceed through the common intermediate OsHCl(H₂)(H₂C=CHF)L₂, via OsClF(=CHMe)L₂ and OsHCl(H₂)(C₂H₄)L₂, all of which are detected. DFT(B3PW91) calculations of the potential energy and free energy at 298 K of possible intermediates show the importance of entropy to account for their thermodynamic accessibility. Calculations of unimolecular C–F cleavage of coordinated C₂H₃F confirms the high activation energy of this process. Catalysis by HF is thus suggested to account for the fast observed reactions, and scavenging of HF with NEt₃ changes the product to exclusively Os(H)₂Cl(CCH₃)L₂. The analogous reaction of Os(H)₃ClL₂ with H₂C=CF₂ produces exclusively OsHFCl(≡CCH₃)L₂ and HF, and the latter is again suggested to catalyze C–F scission via the observed intermediates Os(H)₂Cl(CF₂CH₃)L₂ and OsHCl(=CFMe)L₂.

Introduction

We have reported^{1,2} how Os(H)₃ClL₂ (L = PⁱPr₃) binds olefins H₂C=CHD₀ (D₀ = OR, O₂CR) and then loses 2H and isomerizes these olefins ultimately to the carbyne L₂ClHD₀Os[≡C(CH₃)]. These reactions thus effect C–D₀ bond cleavage, sometimes via an intermediate carbene complex.

Against this background, vinyl fluorides represent an interesting extension of our past olefinic substrates. They are π-acidic η² ligands, the C–F bond is strong, yet there is strong evidence that α-fluoro alkyl ligands are highly activated toward C–F cleavage, particularly by Brønsted or Lewis acids.³ Because an H₂ ligand, potentially accessible from Os(H)₃ClL₂, generally shows Brønsted acid behavior,⁴ this may be an influential second reactivity type to augment the Lewis acidity of the metal in unsaturated Os(H)₃ClL₂. We report here an experimental and computational study of the reactivity of Os(H)₃ClL₂ toward vinyl fluorides.

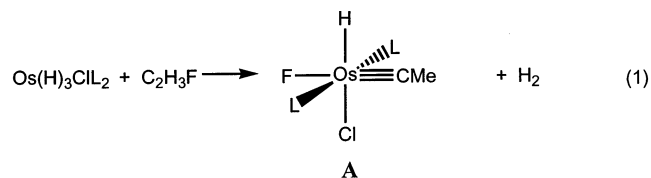
Results

H₂C=CHF as Substrate. (a) General Results. The reaction of Os(H)₃ClL₂ with vinyl fluoride (1:2 mole ratio)

* Authors to whom correspondence should be addressed. Email: caulton@indiana.edu; odile.eisenstein@lsd.univ-montp2.fr.

(1) Coalter, J. N., III; Bollinger, J. C.; Huffman, J. C.; Werner-Zwanziger, U.; Caulton, K. G.; Davidson, E. R.; Gérard, H.; Clot, E.; Eisenstein, O. *New J. Chem.* **2000**, *24*, 9.

in toluene at 20 °C is complete in less than 10 min and proceeds (eq 1) to form H₂ and A.⁵ Compound A is

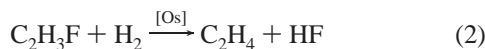


characterized by an upfield resonance in the ¹H NMR spectrum at –6.19 ppm due to the hydride ligand. This signal

- (2) Ferrando, G.; Gérard, H.; Spivak, G. J.; Coalter, J. N., III; Huffman, J. C.; Eisenstein, O.; Caulton, K. G. *Inorg. Chem.* **2001**, *40*, 6610.
 (3) (a) Hughes, R. P. *Adv. Organomet. Chem.* **1990**, *31*, 183. (b) Kiplinger, J. L.; Richmond, T. G.; Osterberg, C. E. *Chem. Rev.* **1994**, *94*, 373. (c) Reger, D. L.; Dukes, M. D. *J. Organomet. Chem.* **1978**, *157*, 67. (d) Michelin, R. A.; Ros, R.; Guadalupi, G.; Bombieri, G.; Benetollo, F.; Chapuis, G. *Inorg. Chem.* **1989**, *28*, 840. (e) Clark, G. R.; Hoskins, S. V.; Roper, W. R. *J. Organomet. Chem.* **1982**, *234*, C9. (f) Crespi, A. M.; Shriver, D. F. *Organometallics* **1985**, *4*, 1830. (g) Koola, J. D.; Roddick, D. M. *Organometallics* **1991**, *10*, 591. (h) Richmond, T. G.; Crespi, A. M.; Shriver, D. F. *Organometallics* **1984**, *3*, 314. (i) Hughes, R. P.; Lindner, D. C.; Rheingold, A. L.; Liable-Sands, L. M. *J. Am. Chem. Soc.* **1997**, *119*, 11544. (j) Hughes, R. P.; Rose, P. R.; Rheingold, A. L. *Organometallics* **1993**, *12*, 3109. (k) Hughes, R. P.; Willemsen, S.; Williamson, A.; Zhang, D. *Organometallics* **2002**, *21*, 3085. (l) Hughes, R. P.; Smith, J. M. *J. Am. Chem. Soc.* **1999**, *121*, 6084. (m) Braun, T.; Noveski, D.; Neumann, B.; Stammmler, H.-G. *Angew. Chem., Int. Ed.* **2002**, *41*, 2745.
 (4) Abdur-Rashid, K.; Fong, T. P.; Greaves, B.; Gusev, B. D.; Hinman, J. G.; Landau, S. E.; Lough, A. J.; Morris, R. H. *J. Am. Chem. Soc.* **2000**, *122*, 9155.

is a triplet of doublets ($J_{(H-P)} = 15.6$ Hz, $J_{(H-F)} = 9.6$ Hz). The $^{31}\text{P}\{^1\text{H}\}$ NMR spectrum shows a doublet with a coupling constant to the cis fluoride of 44 Hz, and the ^{19}F NMR spectrum is a triplet of doublets at -297.6 ppm.

However, as a result of the released H₂, a second reaction (eq 2) is competitive for vinyl fluoride,

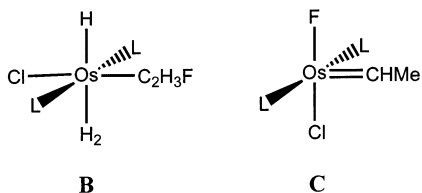


accounting for the stoichiometric production of *free* ethylene (and observed HF: ^1H and ^{19}F NMR evidence). Thus, the overall balanced reaction is eq 3.



Equation 3 is written with unconventional coefficients to clarify the two stoichiometrically linked mechanistic cycles described later. For completeness, we note that, in this reaction, run at either 20 °C or at low temperature (see below), there is no evidence for the species OsH₃ClL₂, OsH₆L₂, OsHCl(olefin)L₂, or OsHCl(=C=CH₂)L₂.

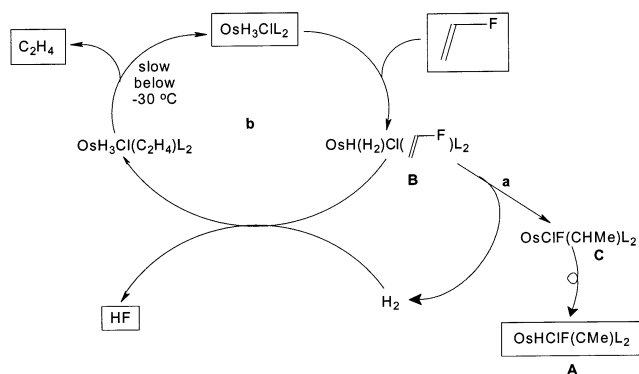
(b) Low-Temperature Monitoring. The competitive character of these two products (alkylidyne **A** and C₂H₄) is best illustrated by a low-temperature reaction of Os(H)₃ClL₂ with excess H₂C=CHF, with subsequent incremental warming of the reaction, while monitoring by ^1H , ^{31}P , and ^{19}F NMR spectra. The first observation in toluene-*d*₈ at -60 °C shows all Os(H)₃ClL₂ has reacted, and the primary product, simple adduct **B**, is characterized by a $^{31}\text{P}\{^1\text{H}\}$ NMR



AB pattern (prochiral olefin), a ^{19}F NMR signal shifted ~ 20 ppm upfield from (visible) free C₂H₃F, and ^1H NMR signals for coordinated vinyl fluoride. Most remarkably, hydride and H₂ in this adduct appear as distinct signals (-4.30 and -14.04 ppm), the former as a triplet. It is noteworthy that the C–F cleavage product² OsHCl(H₂)(C₂H₄)L₂ is already present, as are carbene **C** (^1H , ^{19}F , and ^{31}P NMR evidence; not detected in the rapid reaction at 20 °C) and carbyne **A** (^{19}F , ^1H , and ^{31}P NMR evidence). The persistence of the C₂H₄ adduct in the presence of excess C₂H₃F suggests that the ethylene complex must be an *intramolecular* kinetic product and that replacement of the C₂H₄ ligand by C₂H₃F is kinetically slow. HF is evident by ^1H NMR (11–12 ppm) but better by ^{19}F NMR, which shows at least two broad resonances (-175 and -180 ppm), indicative of HF hydrogen bonded to several different solution species. For example,

(5) The ^1H , ^{31}P , ^{13}C , ^{19}F NMR data for **A** resemble those of OsHCl₂(CMe)L₂. The location of the fluorine trans to carbene was established by the (small) $2J_{\text{H-Os-F}}$, in comparison to reference compounds. See: Huang, D.; Koren, P.; Foltling, K.; Davidson, E. R.; Caulton, K. G. *J. Am. Chem. Soc.* **2000**, *122*, 8916.

Scheme 1



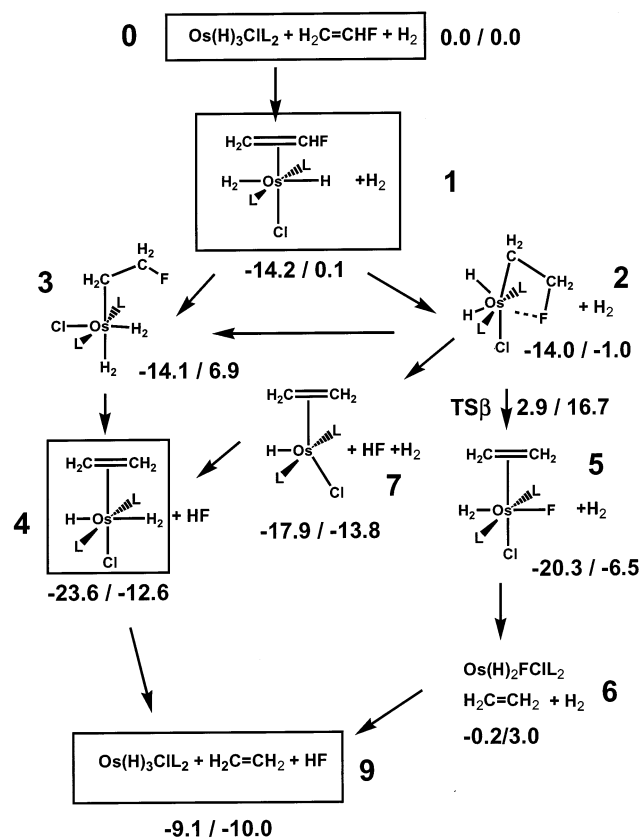
HF has been shown^{6–10} to bind to coordinated F[–]. At -50 and -40 °C, the amount of OsHCl(H₂)(C₂H₃F)L₂ decreases dramatically and OsHCl(H₂)(C₂H₄)L₂ grows. The carbene and carbyne signals do *not* increase in intensity, but two new carbene complexes, OsF₂(=CHMe)L₂ and OsCl₂(=CHMe)L₂, grow in due to halide redistribution. By -30 °C, there is better resolution in the H₂ signal of OsHCl(H₂)(C₂H₄)L₂, so that triplet structure is identifiable, but this ethylene complex still persists, despite available dissolved C₂H₃F. Only at -30 °C is the first trace of free C₂H₄ evident by ^1H NMR at 5.27 ppm. At -20 °C, free ethylene is more abundant (^1H NMR), as are the carbenes and the carbyne **A**. The carbyne Os≡C–CH₃ methyl protons have a distinctive chemical shift, 0.3 ppm. At this temperature, the several ^{19}F NMR signals of “HF” have coalesced to one broad line at -182 ppm. The Os=CH(Me) C_α proton signals attributed to OsCl₂(CHMe)L₂ and OsF₂(CHMe)L₂ grow further.

At $+20$ °C, both the ethylene adduct and the carbene complexes are gone (^1H , ^{31}P , and ^{19}F NMR evidence), there is abundant free C₂H₄, and OsHFCl(CMe)L₂ is the predominant metal-containing product (^1H , ^{31}P , and ^{19}F NMR evidence). HF is evident by both ^1H and ^{19}F NMR spectroscopies. Vacuum removal of all volatiles (to dryness overnight), followed by dissolving the solid residue in toluene-*d*₈ shows that the NMR signals of residual vinyl fluoride, ethylene, and HF are absent. This confirms that hydrogen bonding of HF to OsHFCl(CMe)L₂ can be disrupted by vacuum at 20 °C, and, as a consequence, the carbyne complex ^{19}F NMR chemical shift changes by 4.5 ppm and its ^{31}P NMR chemical shift changes by 1.5 ppm.

The variable-temperature observations and the competitive character of the reaction are accounted for by Scheme 1, where reactants and products are displayed in boxes. All three *intermediate* metal complexes have been detected. The feature which stoichiometrically limits ethylene formation is the production of H₂ by reaction a. In the temperature range -50 to -30 °C, the ethylene complex accumulates,

- (6) Whittlesey, M. K.; Perutz, R. N.; Greener, B.; Moore, M. H. *Chem. Commun.* **1997**, 187.
 (7) Murphy, V. J.; Hascall, T.; Chen, J. Y.; Parkin, G. J. *J. Am. Chem. Soc.* **1996**, *118*, 7428.
 (8) Roe, D. C.; Marshall, W. J.; Davidson, F.; Soper, P. D.; Grushin, V. V. *Organometallics* **2000**, *19*, 4575.
 (9) Jasim, N. A.; Perutz, R. N. *J. Am. Chem. Soc.* **2000**, *122*, 8685.
 (10) Jasim, N. A.; Perutz, R. N.; Foxon, S. P.; Walton, P. J. *Chem. Soc., Dalton Trans.* **2001**, 1676.

Scheme 2. Energies ($E + \text{ZPE}/G(298)$, kcal/mol) of Some Candidates for the Formation of $\text{C}_2\text{H}_4 + \text{HF}$ (Scheme 1, Cycle b)^a



^aArrows represent possible elementary or simple processes

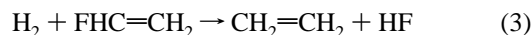
and since (abundant) $\text{C}_2\text{H}_3\text{F}$ can evidently not rapidly replace coordinated ethylene in coordinatively saturated $\text{OsH}_3\text{Cl}(\text{C}_2\text{H}_4)\text{L}_2$, the reaction has reached a metastable steady state. As that substitution occurs, newly formed **B** reacts according to a to generate more H_2 , thus enhancing ethylene production in cycle b. **B** thus represents a branch point and consequently deserves greater scrutiny.

How can **B** branch in two directions to furnish both ethylene and ethylidyne as C–F cleavage products? How can saturated **B** react with H_2 in cycle b?

Computational Studies. To answer these questions and to get some insight into mechanisms that could lead to the observed products, we carried out DFT calculations of possible intermediates and some potential mechanistic steps. P^iPr_3 has been modeled by PH_3 . The intermediates calculated were selected on the basis of previous knowledge^{1,2} of the reactions between RuHClL_2 and an olefin, with addition of two hydrogens in the case of osmium. Two reactions of vinyl fluoride have been considered. One leads to the ethylidyne and H_2 (Scheme 1, path a). The other converts H_2 and vinylfluoride to ethylene and HF (Scheme 1, cycle b).¹¹

Formation of Ethylene from Vinyl Fluoride (Scheme 1, Cycle b). The calculations (Scheme 2) show that the transformation of eq 3 is exoenergetic by 9.1 kcal/mol.

(11) We have also calculated the energy for oxidative addition of the C–F bond of vinyl fluoride to $\text{Os}(\text{H})_3\text{CIL}_2$, to give $\text{OsFClH}_4(\text{C}_2\text{H}_3)\text{L}_2$. This lies 22.2 kcal/mol above the reactants and is thus much less favorable than others described in the schemes which follow.



$\text{Os}(\text{H})_3\text{CIL}_2$ functions as a catalyst for this transformation. Vinyl fluoride coordinates to $\text{Os}(\text{H})_3\text{CIL}_2$ before inserting in one of the Os–H bonds to give a fluoro substituted alkyl ligand. Subsequently, there is the possibility of losing a dihydrogen molecule, HF, or ethylene at different stages of the reaction.

(a) Relative Electronic Energies. Among the intermediates shown in Scheme 2, observed species are enclosed in boxes. The lowest energy stereoisomer of each species has been considered. The geometries of selected minima are given in Figure 1. First, we briefly discuss E , the electronic (or potential) energies (with ZPE corrections) of the various species with respect to the separated reactants $\text{Os}(\text{H})_3\text{CIL}_2 + \text{CH}_2=\text{CHF} + \text{H}_2$, **0**. The coordination of vinyl fluoride is energetically favorable, to form the experimentally observed hexacoordinated 18 e hydrido–dihydrogen olefin complex, **1**. The vinyl fluoride inserts into the Os–H bond leading to a 16 e pentacoordinated β F-ethyl dihydride Os(IV) complex, **2** (note that for convenience, the symbol **2** refers to the Os complex but the energy is that of the Os complex plus that of the associated free molecules: H_2 , HF, etc.). Complex **2** has a C–F bond to be discussed later.

Alternatively, the 16 e species **2** can coordinate H_2 to give a saturated bis-dihydrogen Os(II) complex **3**. Coordination of H_2 to **2** appears to be essentially thermoneutral. From these alkyl complexes **2** or **3**, the cleavage of C–F can lead to a variety of ethylene complexes such as an 18e ethylene hydrido–dihydrogen complex by loss of HF, **4**, or to an 18-electron ethylene fluoro–dihydrogen complex **5** by β -F migration to Os. A 16 e ethylene–hydrido complex **7**, with loss of H_2 and HF, has also been considered. The ethylene complexes **4**, **5**, and **7** are energetically more favorable than the alkyl complexes **2** or **3** and are more stable than the vinylfluoride complex and H_2 , **1**. There is thus a preference for forming the ethylene complex with F going either on the metal center or making HF. System **4** is calculated to be the lowest energy point on the scheme. Loss of the ethylene ligand from **4** produces the final products $\text{Os}(\text{H})_3\text{CIL}_2 + \text{CH}_2=\text{CH}_2 + \text{HF}$, **9**, completing the catalytic conversion of eq 3. The same product **9** can be obtained from **5** via the formation of the dihydride fluoro–chloro 16 e complex, **6**, followed by reaction of H_2 with $\text{Os}(\text{H})_2\text{FCIL}_2$ to make $\text{Os}(\text{H})_3\text{CIL}_2$ plus HF. Complex **6** is calculated to be least stable and thus least probable as a mechanistic participant. The overall reaction from **0** to **9** is energetically downhill and thus favorable. However, several species such as **4** have energies lower than the observed final products. Because formation of the final products requires decoordination with increase in entropy, we now look at the same scheme with Gibbs free energy, G .

(b) Gibbs Free Energies. The free energies, calculated at 298 K, highlight the importance of the entropic contribution. As expected from the fact that **0** and **9** have the same number of independent molecules, inclusion of entropy does not significantly modify their relative energies. In contrast, all other intermediates, which consist of only one or two

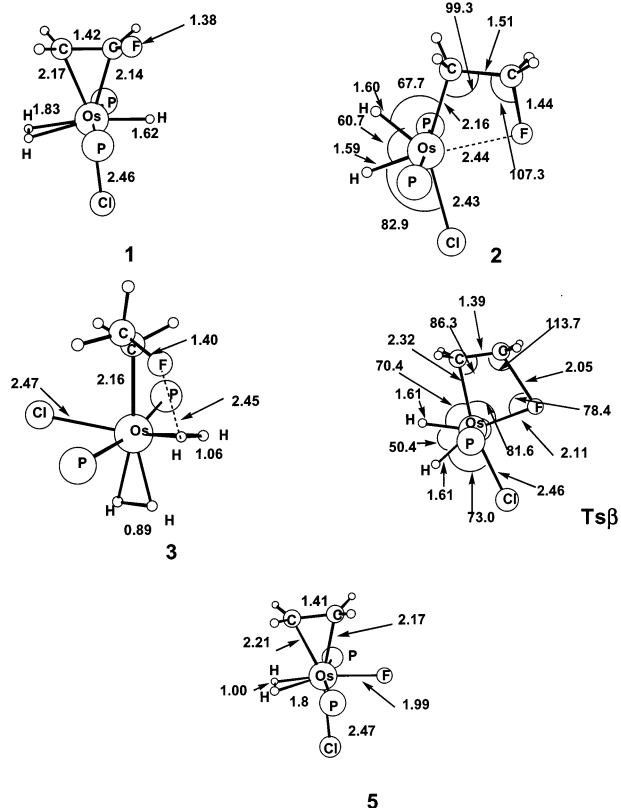
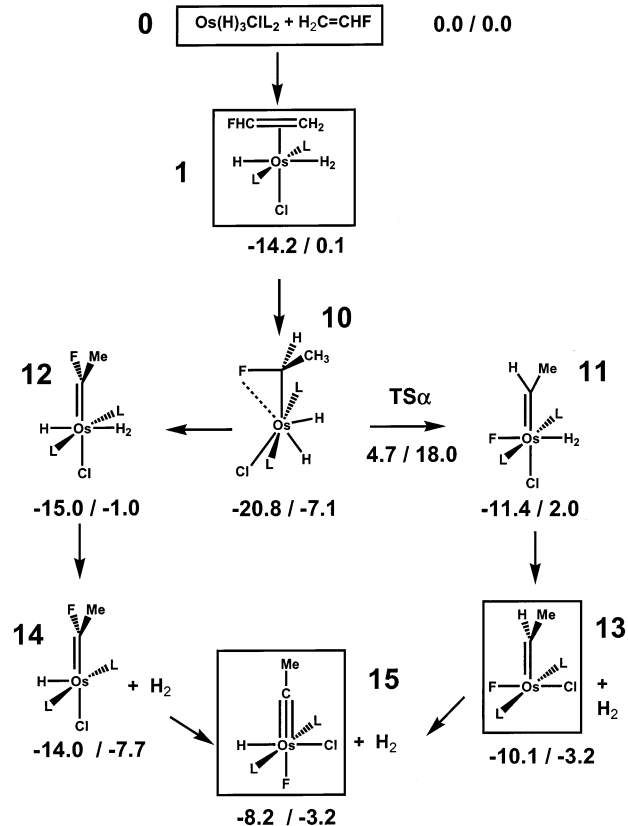


Figure 1. Structures (angstroms, degrees) of selected structures shown on Scheme 2. H from PH_3 are not shown, for clarity.

independent molecules, become much less favorable. Coordination of the olefin becomes energetically essentially neutral. The alkyl complex, **2**, without coordinated H_2 , is isoenergetic with the reactants and coordination of H_2 to give **3** is unfavorable. In these systems where none of the ligands (H_2 or olefin) are strong Lewis bases and where none of the suggested complexes have strong electron deficiency (16 e complexes with at least one π donor ligand), no strong binding (E) energy to the metal center is obtained (average 15 kcal/mol). The entropy thus plays an important role. This has the important consequence that the most stable species on the potential energy surface, **4**, is not a deep free energy well and that loss of ethylene is feasible. This scheme accounts for the observation of **4** at low temperature and **9** at higher temperature.

Forming the Alkylidyne (Scheme 1, Path a). Although we will, in this case, also need to discuss the free energy pattern, it is useful to start with a discussion of the potential energy surface, E . The possible intermediates are shown in Scheme 3, where again boxes enclose observed species. Calculated structures are shown in Figure 2. Pathways through coordination of additional H_2 are not considered since alkylidyne is observed before additional H_2 is released. After coordinating to $\text{Os}(\text{H})_3\text{ClL}_2$ to give **1**, the vinyl fluoride inserts into an Os–H bond to give a 16-electron dihydride α F ethyl complex, **10**. This complex **10** is more stable (by 6 kcal/mol) than the corresponding β F ethyl, **2**. A similar regio-preference was obtained with alkoxy-substituted alkyl complex of RuHClL_2 and $\text{RuH}(\text{CO})\text{L}_2^+$.¹² This 16e dihydride alkyl Os(IV) complex **10** is also more stable than the olefin

Scheme 3. Energies ($E + \text{ZPE/G}(298)$, kcal/mol) of Some Candidates for the Formation of Ethylidyne and H_2 ^a



^a Arrows represent possible elementary or simple processes

complex **1**. From the alkyl complex **10**, F or H can migrate to Os leading to either a non-heteroatom-stabilized carbene, **11**, with an Os–F bond or a F-stabilized carbene complex, **12**. Complex **11** is only slightly less stable than **12**, showing how an Os–F bond replacing an Os–H bond can almost compensate for the C–F σ and (partial) π bonds. Similar energy preferences have already been obtained with a Rh complex and fluoro benzene¹³ and for carbene complexes of Ru.¹⁴ In the two carbene complexes, **11** and **12**, the metal has been reduced because an H_2 ligand has formed. In both of these carbene complexes, H_2 is essentially not bonded to Os as shown by the energies of **13** and **14** being only 1 kcal/mol less stable. Complex **14** is 4 kcal/mol more stable than **13**. Formation of the alkylidyne **15** is slightly endoenergetic from either **13** or **14** (6 kcal/mol). It has been shown in previous computational work that an alkylidyne complex could be significantly stabilized (~ 10 kcal/mol) with respect to the carbene isomer by a more donating phosphine (PMe_3).^{2,15} However, even if better electron-donating phosphine ligands were included in the calculations, this analysis of the potential energy surface reveals that the formation of

- (12) Huang, D.; Bollinger, J. C.; Streib, W. E.; Foltling, K.; Young, V., Jr.; Eisenstein, O.; Caulton, K. G. *Organometallics* **2000**, *19*, 2281.
 (13) Bosque, R.; Clot, E.; Fantacci, S.; Maseras, F.; Eisenstein, O.; Perutz, R. N.; Renkema, K. B.; Caulton, K. G. *J. Am. Chem. Soc.* **1998**, *120*, 12634.
 (14) Gérard, H.; Davidson, E. R.; Eisenstein, O. *O. Mol. Phys.* **2002**, *100*, 533.
 (15) Spivak, G. J.; Coalter, J. N., III; Oliván, M.; Eisenstein, O.; Caulton, K. G. *Organometallics* **1998**, *17*, 999.

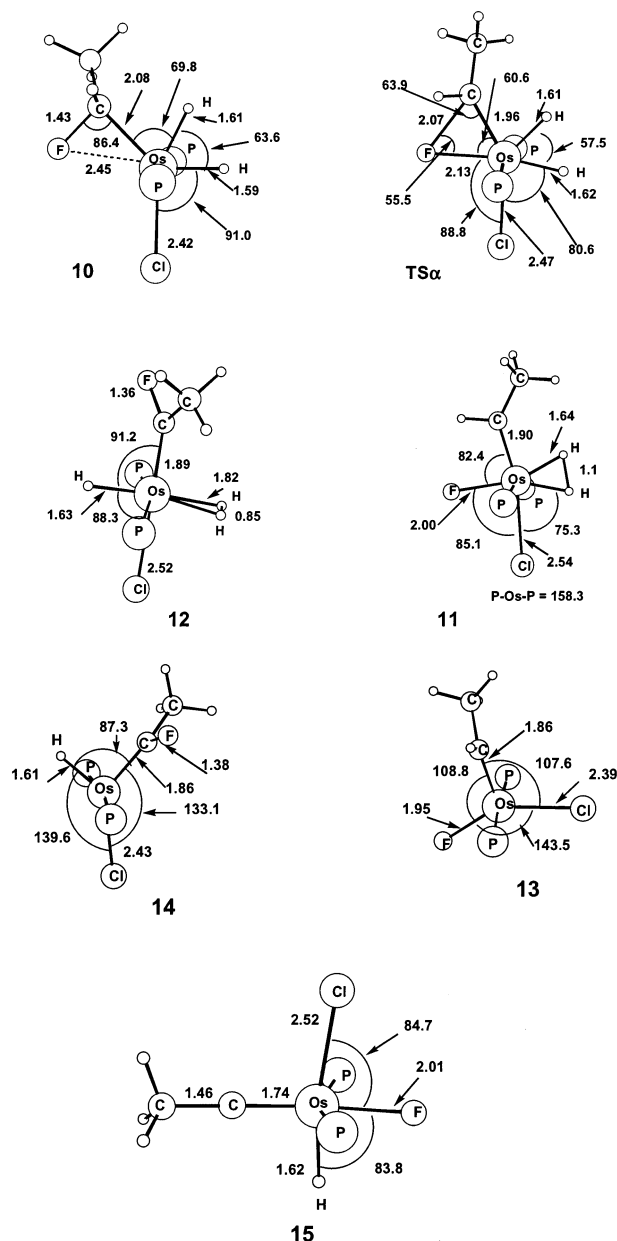


Figure 2. Structures (angstroms, degrees) of selected structures shown on Scheme 3. H from PH_3 are not shown, for clarity.

the alkylidyne is, overall, not energetically very favorable and that species such as **10** and **12** are more favored, especially since this Os(IV) species should be stabilized by a more donating $\text{P}(\text{alkyl})_3$. However, even with PH_3 the final products, **15**, are calculated to be energetically favored over the reactants, **0**.

We go now to the free energies shown in Scheme 3. The number of independent molecules is the same in the reactants and products. This has thus only a small influence on the relative free energies of **0** and **15**. However, several key intermediates that have fewer independent molecules are less favored. In particular, **1** and **10** are brought out of their deep potential energy wells by entropy. Similarly, the free energy of the several carbene complexes is not far from that of **0** or **15**. While the overall free energy pattern suggests that all observed species are thermodynamically accessible, one

should now address the questions of how kinetically accessible are the necessary transformations.

Cleaving the C–F Bond. The transformation of the vinyl fluoride into ethylene, forming **9**, or the formation of **15**, requires at some stage the cleavage of a C–F bond. We know from previous theoretical studies that the activation energy for such transformation is in general high and that C–H cleavage would occur preferentially.¹³ However, we carried out a search for a transition state for the unimolecular cleavage of the C–F bond in the β F-substituted alkyl complex, **2**, and in the α F-substituted alkyl complex, **10**. The transition state for going from **2** to **5** has been located 17.7 kcal/mol (free energy) above **2** (Scheme 2, $\text{TS}\beta$). Likewise, the transition state for the transformation of **10** into **11** is 25.1 kcal/mol (free energy) above **10** (Scheme 3, $\text{TS}\alpha$). The calculated activation free energies are in fact higher than those found in other reactions where it was known that the C–F activation would not occur.¹³ For example, a 16.2 kcal/mol value translates to a half-life of 12 min at -40°C , and a 18.0 kcal/mol value gives a value of 3 h at -40°C . For this reason, we feel these are not viable mechanisms for the observed reactions.

Analysis of Structural Features. (a) F on C_β (Figure 1). Structure **1** has the ligand with the strongest trans influence, H, trans to H_2 . Structure **5** is similar, but with F and H transposed. Complex **2** is an analogue of $\text{Os}(\text{H})_3\text{CIL}'\text{L}_2$ with a β -bonded F serving as L' . This $\text{Os}\cdots\text{F}$ distance is only 0.45 Å longer than the Os–F bond in **5**. The $\text{Os}-\text{C}_\alpha$ and $\text{C}_\alpha-\text{C}_\beta$ distances in **2** are normal, and the C–F bond is slightly lengthened, compared to that in **3**. The $\text{Os}-\text{C}-\text{C}$ bond angle is slightly compressed. $\text{TS}\beta$, linking **2** and **5**, shows considerable Os–F bonding, and major C–F lengthening and C–C shortening. Angle $\text{Os}-\text{C}_\alpha-\text{C}_\beta$ is quite small (86.3°) as this unit becomes an olefin. The two hydrides moved together, but have not formed H_2 , or begun to rotate to take on the H_2 conformation of **5**. Complex **3** is a bis-dihydrogen complex, with a longer H/H distance for the H_2 trans to the π -donor, Cl. The fluorine shows some weak hydrogen bonding to one hydrogen of the stretched H_2 .

(b) F on C_α (Figure 2). **10** also has the shape of $\text{Os}(\text{H})_3\text{CIL}'\text{L}_2$ and shows $\text{F} \rightarrow \text{Os}$ donation to the +4 metal; $\angle\text{Os}-\text{C}-\text{F}$ is compressed to 86.4° . $\text{TS}\alpha$ shows an advanced state of F migration ($\text{C}-\text{F} = 2.07$ Å and $\text{Os}-\text{F} = 2.13$ Å), including some rotation of the emerging carbene CHCH_3 , but little evidence for the coalescence of the two hydrides to H_2 . Compound **11** has an H_2 ligand, and the carbene plane rotated so that it does not compete with H_2 for back-donation from the same metal orbital. The P–Os–P angle is significantly bent¹⁶ to permit better back-donation to the carbene. Compound **12** shows little back-donation to H_2 because it is trans to a hydride ligand; the carbene and H_2 use different d orbitals for back-donation. Compounds **13** and **14** have the distinct geometries known¹⁷ when a chloride is replaced by a hydride. While **13** can naturally transform to **15** by α -H

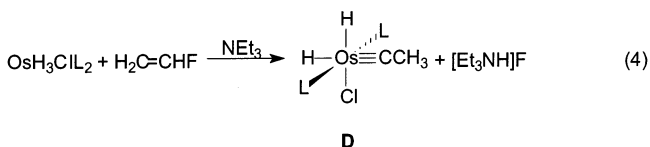
(16) Gérard, H.; Clot, E.; Eisenstein, O. *New J. Chem.* **1999**, *23*, 495.

(17) Riehl, J. F.; Jean, Y.; Eisenstein, O.; Péliissier, M. *Organometallics* **1992**, *11*, 729.

migration, an elementary process cannot move F in **14** to the site trans to carbon.

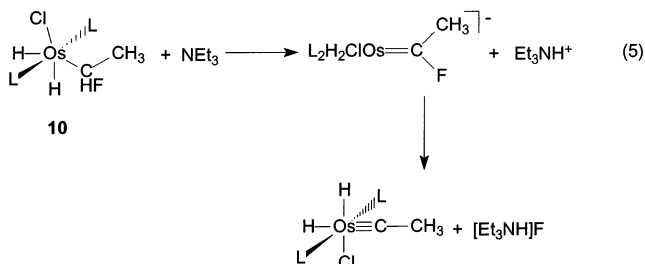
Alternative Mechanism for C–F Cleavage: HF Catalysis. The experimental studies show HF to be present as low as –60 °C, and this permits mechanistic alternatives to those unimolecular reactions explored computationally.¹⁸ Indeed, there is ample experimental evidence that HF hydrogen bonds to various intermediates, so its effective “local” concentration is high. Thus, since the transition states for the conversions **10** → **11** and the dichloro analogue of **13** → **15**¹⁵ are calculated to be quite high, we propose the path through **12** to **14**, with the **14** → **15** conversion being HF-catalyzed. The experimental *observation* of some **13** confirms that its α-H migration conversion to **15** is *not* facile. Conversely, given the thermodynamic accessibility of **14**, its *not* being observed ensures that there is some mechanism for its rapid consumption; this we assert is HF catalysis.^{3i,k,l} We have previously demonstrated that this is the mechanism of migration of PhO– from carbon to osmium in HClOs=[C(OPh)CH₃]L₂.² The removal of F from C_α in **10** will also be HF catalyzed.

To test the hypothesis of HF elimination and catalysis, the reaction of Os(H)₃ClL₂ and H₂C=CHF was repeated in the presence of 1 equiv of NEt₃ in C₆D₆ at 25 °C, with the intention of trapping free HF. In this case, the only product of this rapid (10 min) reaction (eq 4) is Os(H)₂Cl(≡CCH₃)-L₂ (**D**). This compound is characterized in the hydride region



of the ¹H NMR spectrum by two triplets of doublets (coupling to phosphines and to each other) of equal intensity at –6.30 and –12.83 ppm due to inequivalent hydrides. The carbyne protons appear as a broad triplet at 0.96 ppm, and the phosphine methyls show two overlapped apparent quartets, indicating that the phosphines are transoid and the methyls diastereotopic. The ³¹P{¹H} NMR spectrum is a singlet. No signals are observed in the ¹⁹F NMR spectrum because [Et₃NH]F is insoluble in benzene. No other isomers of **D** are observed.

We suggest that NEt₃ directly intercepts the α-fluoro ethyl complex **10**, as shown in eq 5, and that the resulting deprotonated anion is so electron-rich at Os that the ammonium cation can readily abstract fluoride. In this way, the

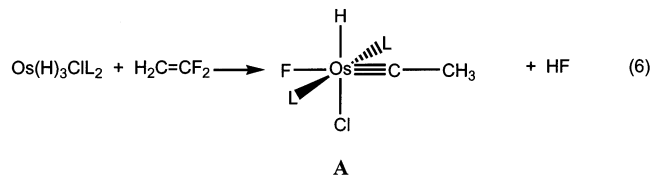


mechanism is diverted at an early stage, and no H₂ is

released, so the ethylene-forming cycle **b**, Scheme 1, is inoperative. Significantly, ethylene is absent in this rapid reaction in the presence of NEt₃. NEt₃ thus intercepts **10**, so it halts production of H₂, and thus the ethylene production is halted.

Subsequently (4 days to completion), all Os(H)₂Cl(CMe)-(PⁱPr₃)₂ disappears and OsHFCl(CMe)(PⁱPr₃)₂ becomes the major (>80%) product. This is a slow reaction attributed to the (weak) acidity of insoluble [Et₃NH]F.

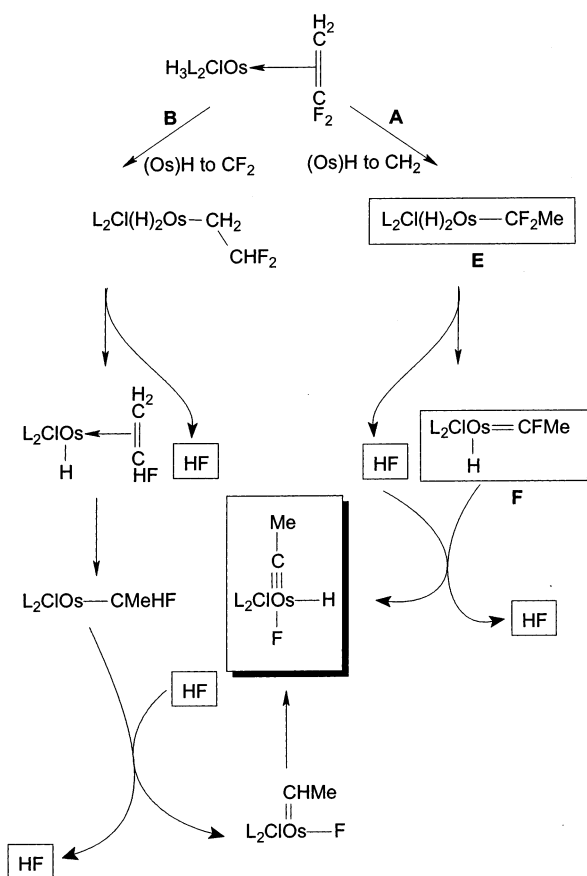
H₂C=CF₂ as Substrate. (a) Room-Temperature Reaction. The reaction of Os(H)₃ClL₂ with H₂C=CF₂ at 20 °C in C₆D₆ occurs in the time of mixing according to eq 6. No



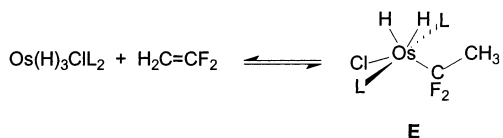
ethylene, vinyl fluoride, or ethyl fluoride are detected. The ¹⁹F NMR spectrum at 20 °C shows a peak due to HF (400 Hz broad singlet) at –184 ppm, which is somewhat shifted from its value reported above; the ¹⁹F chemical shift of OsHClF(CCH₃)L₂ is also shifted 2 ppm from its value reported above. We attribute both of these observations to hydrogen bonding of HF to the F ligand in **A**, but in the dynamic exchange regime at 20 °C. A weak doublet of quartets pattern in the ¹⁹F NMR spectrum at –109 ppm, confirmed via a ¹H NMR multiplet at 5.6 and 0.2 ppm, establishes¹⁹ this *low-yield* product as a trace of F₂CHCH₃. Several mechanisms for forming these products are shown in Scheme 4. The general principles used in this scheme reflect the known chemistry of Os(H)₃ClL₂, together with a principle established from DFT calculations described above and on RuClH(C₂H₃F)(PH₃)₂ and experiments on Os analogues: avoiding unimolecular migration of F from either C_α or C_β in unsaturated d⁶ metal/fluoroethyl species, OsC₂H_{5–n}F_n (n = 1, 2). As described above and in ruthenium analogues, these reactions have been shown to have surprisingly high activation energy, which has been traced to repulsions between metal d electrons and lone pairs on the migrating fluorine. These two points still permit two mechanisms, which differ in the initial step from the olefin adduct by hydride on Os migrating either to the CH₂ carbon (Scheme 4, path c) or to the CF₂ carbon (Scheme 4, path d). Since no intermediates were detected at 20 °C, we do not know which of these initial steps is faster. The detection of trace amounts of H₃CCHF₂ in a low-yield side reaction can be accommodated by H–C(sp³) elimination from either step c or step d. Path d involves a 14-electron species (i.e., OsCl-(CMeHF)L₂), while path c does not. Finally, only path d passes through a vinyl fluoride adduct. In an attempt to choose between path c and path d, the reaction was monitored beginning at low temperature.

(18) This reaction must either depend, for initiation on some progress around the cycle forming ethylene and HF or some adventitious acid catalysis.
 (19) Hudlicky, M.; Pavlath, A. E. *Chemistry of Organic Fluorine Compounds II*; American Chemical Society: Washington, D. C., 1995.

Scheme 4

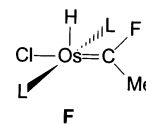


(b) **Low-Temperature Reaction Monitoring.** When $\text{Os}(\text{H})_3\text{ClL}_2$ and $\text{H}_2\text{C}=\text{CF}_2$ (mole ratio $\sim 1:2$) are combined at -196°C , and thawed quickly, the ^1H , $^{31}\text{P}\{^1\text{H}\}$ and ^{19}F spectra at -60°C show 70% conversion to an intermediate of structure **E**. The phosphines are equivalent, but their ^iPr



methyls are diastereotopic. The hydrides are a coalesced apparent triplet at -11.6 ppm, and the ^{19}F NMR spectrum shows one signal ($\nu_{1/2} = 100$ Hz at -40°C) for equivalent fluorines; the coordinated alkyl is *not* in rapid exchange with the small amount of free $\text{H}_2\text{C}=\text{CF}_2$ observed at -81.7 ppm. An apparent triplet is observed by ^1H NMR at 1.65 ppm and is assigned to the methyl protons of the coordinated alkyl. At -50°C , the hydride signal has resolved into five lines, which are assigned as a triplet of triplets with $J_{\text{PH}} \approx J_{\text{FH}} \sim 12$ Hz. The $^{31}\text{P}\{^1\text{H}\}$ NMR signal has resolved into a triplet ($J_{\text{PF}} = 14$ Hz). This coupling constant is too small for F on Os. The ^{19}F NMR spectrum now shows the first traces of *two* signals (-173.2 and -181.0 ppm, unequal intensity), each a doublet with $J_{\text{HF}} = 450$ and 420 Hz, respectively, due to molecular HF differentiated by being hydrogen bonded to two different partners. Each has a half-width of about 100 Hz. At -40°C , there are the beginnings of growth of new peaks which become more clearly evident at -30°C : a

hydride peak (-6.1 ppm), a ^{31}P doublet, a ^{19}F peak (-290 ppm), and an $\text{Os}\equiv\text{C}-\text{CH}_3$ peak at $+0.3$ ppm, all assigned to **A**. At the same time, a set of weak $\text{Os}-\text{H}$, ^{31}P and ^{19}F NMR peaks is also seen; a large $^2J_{\text{HosF}}$ value of ~ 80 Hz is consistent with *trans* stereochemistry,⁵ and this is assigned to the *isomer* of carbyne complex **A** where F is *trans* to hydride, not to the carbyne carbon. A key additional observation is of an intermediate **F** that, at both -40 and -30°C , is more abundant than **A**. This species shows (-30



$^\circ\text{C}$) a 20 Hz ^1H NMR doublet at 1.59 ppm, a strong $^{31}\text{P}\{^1\text{H}\}$ NMR signal (multiplet) at 20.4 ppm, and a strong hydride peak at -9.9 ppm. It is assigned structure **F**; a ^{19}F NMR signal at $+143$ ppm is consistent with fluorine on the carbene carbon. At -30°C , the first *proton* NMR evidence for “HF” is seen as a very broad peak (~ 1 ppm full width at half-height) at $+12$ ppm; this is confirmed by a strong ^{19}F NMR peak at -184 ppm, which is now coalesced and shows none of the multiplicity evident at lower temperatures. At this temperature, the alkyl **E** constitutes only about 30% of the signal intensity of **A** and **F**. At -20°C and above, **E** is gone and **F** declines dramatically, all with formation of **A**. Already at -20°C , the ^1H NMR due to “HF” has sharpened somewhat at $+11.2$ ppm (0.5 ppm half-width), as does its ^{19}F NMR signal at -182 ppm. There is no significant change at -10°C or at $+10^\circ\text{C}$, indicating that the reaction has gone to completion according to eq 6.

The detection of **E** and **F** permits choosing path c of Scheme 4 as operative. For clarity in Scheme 4, observed species are enclosed in rectangles. This is supported by the DFT computational result that an α -fluoro alkyl is thermodynamically more stable than a β -fluoro alkyl (i.e., the migration of $(\text{Os})\text{H}$ to CH_2 of the olefin is thermodynamically favored). It is also true that there is no trace observed experimentally of the proton on C_α in an $\text{Os}=\text{CH}(\text{Me})$ functionality (at its distinctive chemical shift of $+13$ to $+22$), which argues *against* path d.

Why does the $\text{H}_2\text{C}=\text{CF}_2$ reaction fail to give any ethylene? In fact, path c of Scheme 4 has no species readily converted to ethylene, or even to vinyl fluoride. In addition, the scheme lacks a coordinated dihydrogen. This dihydrogen, when present, is the key to C–F bond cleavage in coordinated $\text{H}_2\text{C}=\text{CHF}$; when H_2 is absent, as in the $\text{H}_2\text{C}=\text{CF}_2$ reaction, this step in cycle b of Scheme 1 is impossible, and $\text{H}_2\text{C}=\text{CH}_2$ cannot be formed. In short, the $\text{H}_2\text{C}=\text{CF}_2$ reaction fails to give ethylene (or vinyl fluoride) since the hydride-to-F ratio is lower than when $\text{H}_2\text{C}=\text{CHF}$ reacts with $\text{Os}(\text{H})_3\text{ClL}_2$.

Conclusions

Origin of the Barrier. Why is the energy barrier for α - or β -migration of F so high? It has been shown that one reason for the high-energy barrier for cleaving a α C–F bond

was the presence of a destabilizing interaction between an occupied metal d orbital and one of the lone pairs of F.¹⁵ This computational analysis was carried out on the transformation of RuClL₂(CH₂F) to RuClFL₂(CH₂).¹⁴ In the present case, we have a related reaction (**10** to **11**), which transforms Os(H)₂ClL₂(CHFMe) into Os(H₂)ClL₂(CHMe). The difference from the Ru case is two additional H ligands and thus two fewer d electrons in the plane perpendicular to the P/P line. The geometries of the Os–C–F triangle in TS α for Os and Ru are very similar. Despite this, the activation barrier remains paradoxically high. One possible reason is that a d orbital used for the Os–H bonds is necessary for making the Os–C(carbene) π bond. The d electrons could have been made available by internal redox, via the formation of an H₂ ligand from the two hydride ligands. However, this transformation would have created a destabilizing interaction between the F lone pair and the occupied d orbital. It thus appears that there is no good solution to stabilize the TS. Either Os(IV) becomes Os(II) and a strong destabilization with F occurs or it stays Os(IV) and fails to create the new Os–C π bond. There is either a strong antibonding interaction or lack of bonding interaction at the TS, which keeps it at high energy.

C–F Cleavage Mechanism. These results show very facile C–F bond cleavage by Os(H)₃ClL₂, but the actual cleavage event seems to require Brønsted acid catalysis, rather than facile unimolecular migration of F from carbon to Os; F migration appears to be much less facile than is the corresponding β -H migration. Even a 1,2-F migration to Os in the alkyl OsCFXR (X = H or F) unit appears to have a high barrier, as indicated by an extensive study of a ruthenium analogue and confirmed here by new computational results. Once some HF is liberated, then its action becomes autocatalytic. It is this reagent that so completely removes F from carbon in the two vinyl fluorides studied here, consistently producing an osmium carbyne. Thus, H₂C=CF₂ gives only the carbyne, while the singly fluorinated carbon in H₂C=CHF is subject to competitive conversion to ethylene. HF thus plays a key role in rapidly bringing these reactions to thermodynamic equilibrium. With vinyl fluoride as substrate, hydrogenolysis of the C–F bond is more exergonic than is formation of the carbyne, but the latter is a reaction in a hydrogen-depleted environment (compare the stoichiometries of eqs 1 and 2).

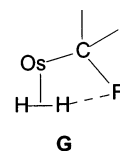
Computational Insights. The DFT calculations provide the following conclusions, which advance understanding of the reaction:

(a) Cycle b of Scheme 1 is thermodynamically favorable, providing a 10 kcal/mol free energy yield, but its occurrence waits for production of H₂ by competing process a in Scheme 1. Process a (see also Scheme 3) is nearly thermoneutral, and thus depends on cycle b of Scheme 1 (and acid catalysis) to make it occur to completion.

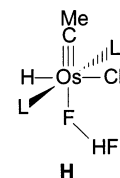
(b) The species OsH₂Cl(C₂H₄F)L₂, **2** and **10**, are both alkyl dihydrides, and structural analogues of Os(H)₃ClL₂, and both are thermodynamically accessible from key species **B** (Scheme 1), although the isomer with F on C α (**10**) is more stable (by about 7 kcal/mol) than **2**.

(c) The binding of H₂ to both carbenes OsXCIL₂(CYMe), (X, Y = H, F), **13**, **14**, is extremely weak, and this is the step in a (Scheme 1) where H₂ is produced, for use there in cycle b.

Returning to the introduction of this paper, although we considered here computationally numerous mechanisms wherein Brønsted acidic coordinated H₂ promoted HF elimination (**G**), we are forced to conclude that this is not effective here in C–F bond cleavage, primarily because H₂ does not bind strongly to these metal complexes (complex **12** \rightarrow **14** or **11** \rightarrow **13**) or is in a dihydride form (and thus less acidic, complex **10**). A reaction from **G** may only be the *initial* source of HF, which is then regenerated in the autocatalytic process.



The possibly surprising persistence of the hydride in OsHCIF(CMe)L₂ in the presence of HF, that is the *lack* of conversion to H₂ and OsClF₂(CMe)L₂, shows that this hydride is inert toward HF. Indeed, OsHCIF(CMe)L₂ *does* interact with HF, but by formation of **H**, so the most Brønsted basic site on OsHCIF(CMe)L₂ is the *fluoride*.



Throughout this study, DFT calculations have shown that the usual migration/insertion steps are kinetically “unviable”, and thus other routes have to be considered. In certain reactions, calculated reaction energies are positive for reactions which are observed to occur. In these reactions in particular, free HF will aggregate with itself, in addition to with metal complexes, subtly altering the thermodynamics calculated here and contributing further stability to reactions which liberate HF.

Experimental Section

General Considerations. All manipulations were performed using standard Schlenk techniques or in an argon filled glovebox unless otherwise noted. Solvents were distilled from Na, Na/benzophenone, P₂O₅, or CaH₂, degassed prior to use, and stored over 4 Å molecular sieves in airtight vessels. All reagents were used as received from commercial vendors after drying and degassing when necessary. ¹H NMR chemical shifts are reported in parts per million relative to protio impurities in the deuterio solvents. ³¹P NMR spectra are referenced to an external standard of 85% H₃PO₄ (0 ppm). ¹⁹F NMR spectra are referenced to an external standard of CF₃COOH (–78.5 ppm vs CFCl₃). Valved NMR tubes were equipped with Wilmad Teflon liners to avoid broadening of the ¹⁹F signals and glass damage due to interaction of liberated HF with the glass walls. NMR spectra were recorded with either a Varian Gemini 2000 (300 MHz ¹H; 121 MHz ³¹P; 75

MHz ^{13}C ; 282 MHz ^{19}F), a Varian Unity Inova instrument (400 MHz ^1H ; 162 MHz ^{31}P ; 101 MHz ^{13}C ; 376 MHz ^{19}F), or a Varian VXR instrument (400 MHz ^1H ; 101 MHz ^{13}C). The following abbreviations are used: s = singlet, d = doublet, dd = doublet of doublets, dt = doublet of triplets, t = triplet, td = triplet of doublets, q = quartet, vt = virtual triplet, dvt = doublet of virtual triplets, m = multiplet, br = broad, ap = apparent.

Reaction of $\text{Os}(\text{H})_3\text{Cl}(\text{P}^i\text{Pr}_3)_2$ and Vinyl Fluoride at 20 °C.

In an NMR tube, $\text{Os}(\text{H})_3\text{Cl}(\text{P}^i\text{Pr}_3)_2$ (0.01 g, 0.018 mmol) was dissolved in 0.5 mL of toluene- d_8 . The solution was frozen and the headspace evacuated. Vinyl fluoride (302 mmHg, 0.036 mmol) was vacuum transferred to the headspace, and the solution was allowed to thaw. The reaction is immediate judging from the strong effervescence observed. The products in solution are the hydrido-carbynes $\text{OsHCl}_2(=\text{CCH}_3)(\text{P}^i\text{Pr}_3)_2$ ⁵ and $\text{OsHFCl}(=\text{CCH}_3)(\text{P}^i\text{Pr}_3)_2$. ^1H NMR (400.1 MHz, C_7D_8 , 20 °C): δ -6.19 (td, $J_{(\text{H}-\text{P})} = 15.6$ Hz, $J_{(\text{H}-\text{F})} = 9.6$ Hz, Os-H, 1H), 0.43 (br, Os=C-CH₃, 3H), 1.22 (dvt, $N = 20.1$ Hz, Os-P(CH(CH₃)₂)), 1.30 (dvt, $N = 21.9$ Hz, Os-P(CH(CH₃)₂)), 2.54 (m, Os-P(CH(CH₃)₂)). ^{31}P { ^1H } NMR (162.0 MHz, C_7D_8 , 20 °C): δ 35.4 (d, $J_{(\text{P}-\text{F})} = 44$ Hz). ^{19}F NMR (376.5 MHz, C_7D_8 , 20 °C): δ -297.6 (td, $J_{(\text{F}-\text{P})} = 43$ Hz, $J_{(\text{H}-\text{F})} = 11$ Hz, Os-F). ^{13}C { ^1H } NMR (125.7 MHz, C_7D_8 , 25 °C): δ 19.1 (s, Os-P(CH(CH₃)₂)), 20.5 (s, Os-P(CH(CH₃)₂)), 23.4 (vt, $N = 12.6$ Hz, Os-P(CH(CH₃)₂)), 38.3 (d, $J_{(\text{C}-\text{F})} = 12.6$ Hz, Os=C-CH₃), 241.8 (br, Os=C).

Reaction of $\text{Os}(\text{H})_3\text{Cl}(\text{P}^i\text{Pr}_3)_2$ and Vinyl Fluoride at Low Temperatures.

In an NMR tube, $\text{OsH}_3\text{Cl}(\text{P}^i\text{Pr}_3)_2$ (0.0169 g, 0.031 mmol) was dissolved in 0.5 mL of toluene- d_8 . The solution was frozen and the headspace evacuated. Vinyl fluoride (250 mmHg, 0.035 mmol) was vacuum transferred to the headspace. The NMR tube was stored at -78 °C for 5 min and placed in a precooled probe at -60 °C. The temperature was raised in 10 °C increments, and the reaction was allowed to proceed for 10 min at each temperature prior to ^1H , ^{31}P { ^1H }, and ^{19}F NMR acquisition. Only diagnostic data are reported for the observed intermediates. Data for $\text{OsH}_3\text{Cl}(\eta^2\text{-H}_2\text{C}=\text{CHF})(\text{P}^i\text{Pr}_3)_2$. ^1H NMR (400.1 MHz, C_7D_8 , -50 °C): δ -4.30 (t, $J_{(\text{H}-\text{P})} = 22$ Hz, Os-H, 1H), -14.04 (br, Os-(H₂), 2H), 2.98, 6.90 (br, Os($\eta^2\text{-H}_2\text{C}=\text{CHF}$), 3H). ^{31}P { ^1H } NMR (162.0 MHz, C_7D_8 , -50 °C): δ 16.3, 16.7 (AB, $J_{(\text{P}-\text{P})} = 160$ Hz). ^{19}F NMR (376.5 MHz, C_7D_8 , -50 °C): δ -158.1 (d, $J_{(\text{F}-\text{H})} = 79$ Hz, Os($\eta^2\text{-H}_2\text{C}=\text{CHF}$)). Data for $\text{OsH}_3\text{Cl}(\eta^2\text{-H}_2\text{C}=\text{CH}_2)(\text{P}^i\text{Pr}_3)_2$. ^1H NMR (400.1 MHz, C_7D_8 , -40 °C): δ -4.03 (t, $J_{(\text{H}-\text{P})} = 21$ Hz, Os-H, 1H), -14.77 (t, $J_{(\text{H}-\text{P})} = 13$ Hz, Os-(H₂), 2H), 2.76, 2.91 (br AB, $J_{(\text{H}-\text{H})} = 11$ Hz, Os($\eta^2\text{-H}_2\text{C}=\text{CH}_2$), 4H). ^{31}P { ^1H } NMR (162.0 MHz, C_7D_8 , -40 °C): δ 15.2. Data for $\text{OsFCl}(=\text{CHCH}_3)(\text{P}^i\text{Pr}_3)_2$. ^1H NMR (400.1 MHz, C_7D_8 , -30 °C): δ 1.55 (d, $J_{(\text{H}-\text{H})} = 7.5$ Hz, Os(=CHCH₃), 3H), 17.00 (d, $J_{(\text{H}-\text{F})} = 22$ Hz, Os(=CHCH₃), 1H). ^{31}P { ^1H } NMR (162.0 MHz, C_7D_8 , -30 °C): δ 43.2. ^{19}F NMR (376.5 MHz, C_7D_8 , -30 °C): δ -269.9 (br). Data for $\text{OsCl}_2(=\text{CHCH}_3)(\text{P}^i\text{Pr}_3)_2$. ^1H NMR (400.1 MHz, C_7D_8 , -30 °C): δ 19.61 (br, Os(=CHCH₃), 1H). ^{31}P { ^1H } NMR (162.0 MHz, C_7D_8 , -30 °C): δ 43.7. Data for $\text{OsF}_2(=\text{CHCH}_3)(\text{P}^i\text{Pr}_3)_2$. ^1H NMR (400.1 MHz, C_7D_8 , -30 °C): δ 18.25 (br, Os(=CHCH₃), 1H).

Reaction of $\text{Os}(\text{H})_3\text{Cl}(\text{P}^i\text{Pr}_3)_2$ and Vinyl Fluoride in the Presence of NEt_3 .

In an NMR tube, $\text{OsH}_3\text{Cl}(\text{P}^i\text{Pr}_3)_2$ (0.01 g, 0.018 mmol) was dissolved in 0.5 mL of benzene- d_6 , and triethylamine (2.7 iL, 0.018 mmol) was added to the solution via syringe. The solution was frozen and the headspace evacuated. Vinyl fluoride (250 mmHg, 0.035 mmol) was vacuum transferred to the headspace. The reaction is immediate judging from the color change from dark brown to pale brown. After 10 min. the only organometallic compound observed by ^1H , ^{31}P { ^1H } NMR is the dihydride

$\text{OsH}_2\text{Cl}(=\text{C}-\text{CH}_3)(\text{P}^i\text{Pr}_3)_2$. ^1H NMR (400 MHz, C_6D_6 , 20 °C): δ -6.30 (td, $J_{(\text{H}-\text{P})} = 27$ Hz, $J_{(\text{H}-\text{H})} = 8$ Hz, Os-H, 1H), -12.83 (td, $J_{(\text{H}-\text{P})} = 16$ Hz, $J_{(\text{H}-\text{H})} = 8$ Hz, Os-H, 1H), 0.96 (brt, $J_{(\text{H}-\text{P})} = 3$ Hz, Os=C-CH₃, 3H), 1.36 (dvt, $N = 22$ Hz, Os-P(CH(CH₃)₂)), 1.38 (dvt, $N = 22$ Hz, Os-P(CH(CH₃)₂)), 2.18 (m, Os-P(CH(CH₃)₂)). ^{31}P { ^1H } NMR (162 MHz, C_6D_6 , 20 °C): δ 42.7 (s). After 4 days at room temperature all is converted to the carbyne $\text{OsHFCl}(=\text{CCH}_3)(\text{P}^i\text{Pr}_3)_2$.

Reaction of $\text{Os}(\text{H})_3\text{Cl}(\text{P}^i\text{Pr}_3)_2$ and Vinylidene Fluoride at Room Temperature.

In an NMR tube, $\text{OsH}_3\text{Cl}(\text{P}^i\text{Pr}_3)_2$ (0.010 g, 0.018 mmol) was dissolved in 0.5 mL of toluene- d_8 . The solution was frozen and the headspace evacuated. Vinylidene fluoride (250 mmHg, 0.035 mmol) was vacuum transferred to the headspace. The reaction is immediate on warming to 25 °C judging from the color change, and the only organometallic product observed after 10 min is the reported carbyne $\text{OsHFCl}(=\text{CCH}_3)(\text{P}^i\text{Pr}_3)_2$.

Reaction of $\text{OsH}_3\text{Cl}(\text{P}^i\text{Pr}_3)_2$ and Vinylidene Fluoride at Low Temperatures.

In an NMR tube, $\text{OsH}_3\text{Cl}(\text{P}^i\text{Pr}_3)_2$ (0.016 g, 0.029 mmol) was dissolved in 0.5 mL of toluene- d_8 . The solution was frozen and the headspace evacuated. Vinylidene fluoride (400 mmHg, 0.056 mmol) was vacuum transferred to the headspace. The NMR tube was stored at -78 °C for 5 min and placed in a precooled probe at -70 °C. The temperature was raised in 5 or 10 °C intervals, and the reaction was allowed to proceed for 5 min at each temperature prior to ^1H , ^{31}P { ^1H }, and ^{19}F NMR acquisition. Only diagnostic data are reported for the observed intermediates. Data for $\text{OsH}_2\text{Cl}(\text{CF}_2\text{CH}_3)(\text{P}^i\text{Pr}_3)_2$. ^1H NMR (400.1 MHz, C_7D_8 , -50 °C): δ -11.65 (tt, $J_{(\text{H}-\text{P})} = 12$ Hz, $J_{(\text{H}-\text{F})} = 12$ Hz, Os-H, 2H), 1.05 (dvt, $N = 19$ Hz, Os-P(CH(CH₃)₂)), 1.18 (dvt, $N = 22$ Hz, Os-P(CH(CH₃)₂)), 1.65 (t, $J_{(\text{H}-\text{F})} = 14$ Hz, Os-CF₂CH₃, 3H), 2.37 (m, Os-P(CH(CH₃)₂)). ^{31}P { ^1H } NMR (162.0 MHz, C_7D_8 , -50 °C): δ 32.4 (t, $J_{(\text{H}-\text{F})} = 14$ Hz). ^{19}F NMR (376.5 MHz, C_7D_8 , -30 °C): δ -11.5 (br, $\nu_{1/2} = 100$ Hz, Os-CF₂CH₃). Data for $\text{OsHCl}(=\text{CFCH}_3)(\text{P}^i\text{Pr}_3)_2$. ^1H NMR (400.1 MHz, C_7D_8 , -40 °C): -9.9 (br, Os-H, 1H), 1.59 (d, $J_{(\text{H}-\text{F})} = 20$ Hz, Os=CFCH₃, 3H). ^{31}P { ^1H } NMR (162.0 MHz, C_7D_8 , -40 °C): δ 20.4. ^{19}F NMR (376.5 MHz, C_7D_8 , -40 °C): δ 143 (br, $\nu_{1/2} = 110$ Hz, Os=CFCH₃). Data for $\text{OsHClF}(\text{CCH}_3)(\text{P}^i\text{Pr}_3)_2$. ^1H NMR (400.1 MHz, C_7D_8 , -40 °C): δ -10.65 (br.d, $J_{(\text{H}-\text{F})} = 90$ Hz, Os-H, 1H), 0.33 (br, Os-CCH₃, 3H). ^{31}P { ^1H } NMR (162.0 MHz, C_7D_8 , -40 °C): δ 27.7 (br.). ^{19}F NMR (376.5 MHz, C_7D_8 , -40 °C): δ -328 (br, $\nu_{1/2} = 140$ Hz, Os-F). When warming at room temperature (and already at -10 °C), the only product observed is the carbyne $\text{OsHFCl}(=\text{CCH}_3)(\text{P}^i\text{Pr}_3)_2$.

Computational Details.

The calculations were carried out using the Gaussian 98 set of programs²⁰ within the framework of DFT at the B3PW91 level.²¹ LANL2DZ effective core potentials (quasi-relativistic for the metal centers) were used to replace the 60 innermost electrons of Os²² and the 10 core electrons of Cl and

- (20) Frisch, M. J.; Trucks, G. W.; Schlegel, H. B.; Scuseria, G. E.; Robb, M. A.; Cheeseman, J. R.; Zakrzewski, V. G.; Montgomery, J. A., Jr.; Stratmann, R. E.; Burant, J. C.; Dapprich, S.; Millam, J. M.; Daniels, A. D.; Kudin, K. N.; Strain, M. C.; Farkas, O.; Tomasi, J.; Barone, V.; Cossi, M.; Cammi, R.; Mennucci, B.; Pomelli, C.; Adamo, C.; Clifford, S.; Ochterski, J.; Petersson, G. A.; Ayala, P. Y.; Cui, Q.; Morokuma, K.; Malick, D. K.; Rabuck, A. D.; Raghavachari, K.; Foresman, J. B.; Cioslowski, J.; Ortiz, J. V.; Baboul, A. G.; Stefanov, B. B.; Liu, G.; Liashenko, A.; Piskorz, P.; Komaromi, I.; Gomperts, R.; Martin, R. L.; Fox, D. J.; Keith, T.; Al-Laham, M. A.; Peng, C. Y.; Nanayakkara, A.; Gonzalez, C.; Challacombe, M.; Gill, P. M. W.; Johnson, B.; Chen, W.; Wong, M. W.; Andres, J. L.; Gonzalez, C.; Head-Gordon, M.; Replogle, E. S.; Pople, J. A. *Gaussian 98* (Revision A19); Gaussian, Inc.: Pittsburgh, PA, 1998.
- (21) Becke, A. D. *J. Chem. Phys.* **1993**, *98*, 5648. Perdew, J. P.; Wang, Y. *Phys. Rev. B* **1992**, *45*, 13244.
- (22) Hay, P. G.; Wadt, W. R. *J. Chem. Phys.* **1985**, *82*, 299.

P.²³ The associated double ζ basis set was used and was augmented by a d polarization function for Cl and P.²⁴ The other atoms were represented by a 6–31G(d,p) basis set (5d).²⁵ Full geometry optimization was performed with no symmetry restriction, and the

(23) Wadt, W. R.; Hay, P. G. *J. Chem. Phys.* **1985**, *82*, 284.

(24) Hölwarth, H. A.; Böhme, M. B.; Dapprich, S.; Ehlers, A. W.; Gobbi, A.; Jonas, V.; Köhler, K. F.; Stegmann, R.; Veldkamp, A.; Frenking, G. *Chem. Phys. Lett.* **1993**, *208*, 237.

(25) Hariharan, P. C.; Pople, J. A. *Theor. Chim. Acta* **1973**, *28*, 213.

nature of the extrema was assigned by analytical frequency calculations. The potential energies include the ZPE correction. The free energies were calculated at 298 K from harmonic frequency calculations.

Acknowledgment. This work was supported by the National Science Foundation.

IC020365F